Long Range Hydration Effects in Electrolytic Free Suspended Black Films

D. Sentenac* and J. J. Benattar

Service de Physique de l'Etat Condensé, Centre d'Etudes de Saclay, 91911, Gif-sur-Yvette, CEDEX, France
(Received 6 February 1998)

The force law within free suspended black films made of negatively charged aerosol-OT with added LiCl or CsCl is studied accurately using x-ray reflectivity (ca. 1 Å). We find an electrolyte concentration threshold above which a substantial additional repulsion is detected in the LiCl films, up to distances of 100 Å. We interpret this phenomenon as an augmentation of the Debye screening length, due to the local screening of the condensed hydrophilic counterions by the primary hydration shell. [S0031-9007(98)06454-0]

PACS numbers: 68.15.+e, 61.10.−i, 61.20.Qg

Because of their simple geometry and well defined double layered structure, free-standing liquid films made of amphiphilic molecules are remarkable model systems for colloidal science. As an example, the long range stability of films made of neutral surfactants [1], negatively charged surfactants [2], and negatively charged amphiphilic polymers [3] can be well accounted for by simple mean-field electrostatic theories. A more complex situation arises in black films (thicknesses in the range 60–300 Å) drawn from sodium dodecyl sulfate (SDS), which exhibit, upon high addition of sodium chloride [4] or cesium chloride [5], a spectacular thinning transition when the distance between the molecular planes, i.e., the separation, is ≈30 Å. Recently, progress has been made toward the understanding of this thinning transition, where it has been argued that the electrostatic correlations between the ions may be predominant, rather than attractive dispersion forces [5,6]. This transition leads to the formation of the Newton black film, where no liquid water remains in its core [7]. This kind of reversed membrane is stabilized by both hydration and protrusion forces, the latter arising from molecular motion of the surfaces [8]. The nature and magnitude of these forces remain a central question in colloidal science. Their investigation is an extremely difficult task, as they both take place at the molecular level. Studies reported on hydration forces, in systems where protrusion forces do not occur, have revealed a short range behavior (they occur at separation ≲40 Å) and a magnitude regulated by the number of hydration and the concentration of the ions that bind to or condense electrostatically at the surfaces (hard walls in this case) [8]. Complications arise when considering the ion size that also influences the strength of surface forces. Size effects impose an upper limit on the density of the condensed counterions in the vicinity of a charged surface. This can be accounted for in several ways: by the introduction of an exclusion zone for the counterions, also known as the Stern layer [9], by the entropy of mixing [10], or by an ion-ion hard core interaction [11]. Whatever the method used, size effects give rise to an additional repulsion, which is significant beyond the short range level, as they saturate the Debye screening of surfaces. Inter-estingly, ion size in water is related to its hydration radius and therefore steric and hydration effects are interdependent. However, as mentioned above, ion hydration has been reported so far to give rise only to structural short range interactions. We show in this Letter that ion hydration also leads to long range behavior.

We measured accurately the long range force law within a free suspended black film, drawn from an aqueous solution of negatively charged aerosol-OT (AOT) (Sigma, purity >99%) with two types of electrolyte added at high concentrations (0.05, 0.1, and 0.2 M). The electrolytes used are LiCl and CsCl (Fluka purity >99.5%). The two counterions differ significantly in their number of hydration: 5–6 water molecules per Li^+ ion and 1–2 per Cs^+ ion. However in water, Li^+ ions have a hydrated radius of 3.8 Å comparable to 3.3 Å for Cs^+ ions [8]. All of the measurements were performed with a concentration of AOT at the critical micellar concentration (CMC), equal to 2.5 mM. At the CMC, micelles begin to form, and macroscopic films can be stabilized. In all of the systems studied, the added electrolyte concentration is higher than that of the surfactant by several orders of magnitude. The contribution of the AOT self-counterion Na^+ in the interactions can therefore be neglected. Similar to [12] (after several stages of purification), no minimum in the surface tension isotherm of the pure AOT solution was detected. The salts were annealed at 500 °C before use to remove any surface impurities. The water used comes from a milli-Q system. Its surface tension is 72.5 mN/m at 22 ± 1 °C. All measurements were carried out at 22 ± 1 °C.

The force law between the molecular planes follows from the measurements of the disjoining pressure and the equilibrium thickness of the film using a very recent technique. It combines the original porous plate method [13,14] with the accurate determination of the thickness, using x-ray reflectivity [15]. With the introduction of the x rays, this apparatus allows the investigation of forces at the molecular level [16]. The porous plate method uses a porous glass disk as a liquid reservoir for the free-standing

film. A hole drilled through the disk is used as a holder for a horizontal liquid film. The ensemble is enclosed in an airtight Plexiglas cell partially filled with the solution to maintain a saturated vapor atmosphere. A pressure ΔP can be applied on the film by means of a syringe connected to the cell, whereas the porous plate is connected to a capillary tube at the atmospheric pressure P_0 (Fig. 1). The pressure in the cell is $\Delta P + P_0$, and ΔP is measured by means of a differential manometer with an accuracy of 0.1 millibar (mb). The disjoining pressure Π_d of the film is the pressure difference between the film reservoir and the gaseous phase. It is thermodynamically related to the derivative of the Gibbs free energy of the film [17]. Experimentally, it is given by the relation $\Pi_d = \Delta P - P_h$, where $P_h = \Delta \rho g h - 2\sigma/r$ is the hydrostatic pressure, σ is the surface tension of the solution, r is the capillary tube radius, g is the gravitational acceleration, and $\Delta \rho$ is the density difference between the solution and the air. The hydrostatic pressure is of the order of 1 mb and can be neglected in the present study. The maximum pressure allowed is fixed by the Laplace pressure of the pores inside the disk. We used porous plates (Robu) with a mean pore radius of 0.75 μm allowing pressures $\lesssim$600 mb. To achieve an x-ray reflectivity experiment

FIG. 1. Scheme of the apparatus installed in the center of the diffractometer. A macroscopic flat film (15 × 4 mm²) is drawn at the extreme upper surface of the hole of the porous plate initially filled with the solution. The disjoining pressure of the film is measured by the application of an additional pressure in the cell. The film structure is determined by x-ray reflectivity.

in association with disjoining pressure measurements, the films are formed with a modified version of the traditional porous plate. Two hermetically sealed Kapton windows allow the passage of the beam through the cell. The hole size of the disk is macroscopic (15 × 4 mm²) as imposed by the reflection of x rays at grazing angles. In addition, the film must stand on the extreme upper surface of the disk holder. For that purpose the hole profile has an inclination angle of 30°. To avoid any residual shadowing effects due to the meniscus of the film, a slit of 1 μm depth was added in the continuation of the hole, in the direction of the beam.

The cell is placed on the head of a four-circle diffractometer in a horizontal geometry. A conventional fine-focus copper tube is used as an x-ray source. The monochromator is a Si(111) crystal which selects the Cu $K_{\alpha 1}$ line ($\lambda = 1.5405$ Å). The beam is collimated in the scattering plane by an incoming slit (100 μm) placed at 40 cm from the source, providing a low divergence (0.15 mrad). A vertical slit (3 mm) is used to limit the width of the illuminated area on the film. The reflected beam is detected by a scintillation counter placed behind an analysis slit (250 μm) at a distance 40 cm from the center of the diffractometer. The incident and reflected beams pass through vacuum flight paths.

The specular reflectivity exhibits Kiessig fringes resulting from the interference due to large density gradients through the film. A film mosaic arises due to the non-flatness of the holder which broadens the specular peak in the transverse direction by about 20%. Finally, the level of accuracy achieved with this apparatus is $\lesssim$1 Å for the determination of the real thickness of the film. The analysis of the reflectivity profiles is performed rigorously through the use of an optical formalism valid at all angles [18], convoluted with the experimental Gaussian resolution, including the film mosaic. The film is described by a succession of homogeneous slabs in the direction perpendicular to the film, each of them characterized by three parameters: thickness, electron density, and interfacial roughness. The electron density is related to the refractive index via the relation $\rho = 2\pi \delta/\lambda^2 r_e$, where r_e is the classic radius of electron and δ is the so-called reduced density.

The knowledge of the generic structure of AOT black films is the first step for the Π_d-isotherm determination. No structure differences have been detected whatever the electrolyte added, and the thickness of the aqueous core (the separation) is the only adjustable parameter during pressure measurements. Table I shows the parameters corresponding to the best fit of the reflectivity curve recorded on a 44 Å thick 2.5 mM AOT black film with added 0.4 M LiCl. The film is described by a symmetrical 3-layer model distinguishing the aqueous core from the two amphiphilic layers. The interfacial roughnesses are due essentially to the thermal fluctuations of the molecular
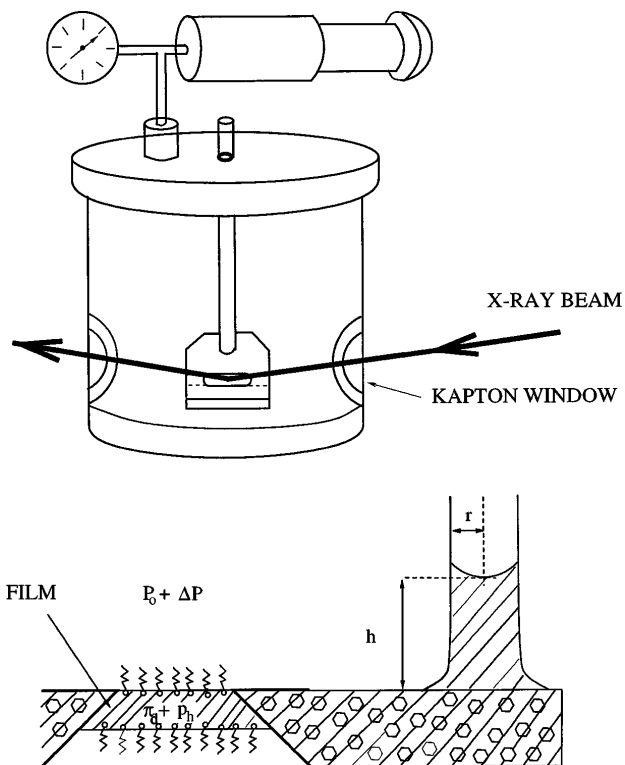
TABLE I. Structural parameters of a symmetrical 3-layer model, as determined by x-ray reflectivity, of a free-standing black film drawn from a solution of AOT (2.5 mM) with added 0.4 M LiCl. The total thickness is 44 ± 1 Å.

Region	Reduced density $(\delta \times 10^6)$	Thickness (Å)	Roughness (Å)
AOT layer	4.2 ± 0.1	11 ± 0.5	3.3 ± 0.5
Aqueous core	3.68	22 ± 0.5	3.3 ± 0.5

layers [7]. The contribution of the two surfactant planes to the overall thickness is 22 ± 1 Å.

The pressure was increased by steps of 50 mb (until film rupture) every 30 mn to ensure the film is in equilibrium. The films remain entirely homogeneous over their whole area and react instantaneously to any pressure variation. Several successive scans on the LiCl systems are shown in Fig. 2. Note the high contrast of the Kiessig fringes which allow the detection of thickness changes of $\lesssim 1$ Å. The Π_d-isotherms are plotted with respect to the separation between the AOT molecular planes in Fig. 3. One can first notice that the slope of all of the Π_d-isotherms above 0.05 M of salt tends to bend at the lowest pressures ($\lesssim 10^4$ N/m^2). Such an effect has been previously observed on Π_d-isotherms of SDS films with added CsCl [5], and is the signature of the attractive dispersion forces. At 0.05 M the Π_d-isotherms with LiCl or CsCl are identical. At 0.1 M of electrolyte added, an additional repulsion arises on the LiCl Π_d-isotherms up to separations of 100 Å. A similar gap is present at 0.2 M of electrolyte, keeping approximately the same value of

≈ 10 Å up to 100 mb. As a result, the formation of the gap is both electrolyte and concentration dependent. The fact that the film thickness depends on the electrolyte has already been pointed out and is related to the strength of the binding of the counterions in the vicinity of the surface [19,20]. Here, the analysis of the disjoining pressure isotherms allows us to specify the origin of this effect.

The general shape of all of the Π_d-isotherms with Cs$^+$ ions presents a rather good agreement with mean-field electrostatic theory, neglecting size effects [21,22]. The surface potentials fitted at the aqueous core/surfactant interface are in the range 95–100 mV. These potentials are similar to those predicted in [5] for SDS films. However, above 0.1 M the Π_d-isotherms obtained with Li$^+$ ions cannot be accounted for by these theories. Adding a Stern layer of thickness 4 Å (much larger than one would expect relative to a CsCl electrolyte) does increase the electrostatic repulsion but not sufficiently to explain the gap. Moreover, steric effects may already be present in the films containing 0.05 M of electrolyte, which are several orders of magnitude above the CMC. Therefore, the important discrepancy observed cannot be simply due to a finite size effect.

In fact, the gap that arises between the CsCl and LiCl Π_d-isotherms can be directly related to the behavior of the corresponding surface tension isotherms. Figure 4 shows two isotherms of surface tension of an AOT solution containing 0.2 M of LiCl or CsCl. A clear gap can be seen between the two surface tension isotherms indicating a higher adsorption of AOT molecules at the air/solution interface, with Cs$^+$ ions present rather than Li$^+$ ions. In addition, the CMC appears higher in the case of LiCL (0.32 mM) than CsCL (0.15 mM). Much below the
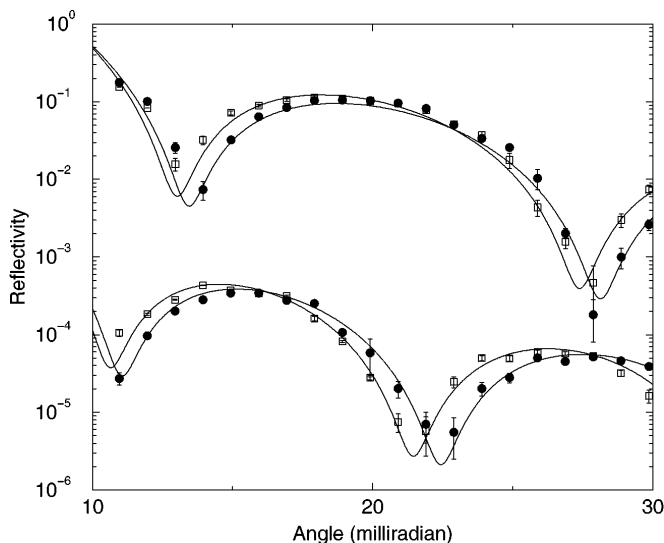

FIG. 2. Successive x-ray reflectivity curves on a black film of AOT (2.5 mM) with added 0.2 M LiCl. Lower curves: $\Delta P = 200$ mb (triangles), $\Delta P = 250$ mb (circles). Upper curves (shifted): $\Delta P = 450$ mb (triangles), $\Delta P = 500$ mb (circles). The theoretical fits are in solid lines and indicate a thinning transition from 72 ± 1 Å to 69 ± 1 Å (lower curves) and from 61.5 ± 0.5 Å to 60 ± 0.5 Å (upper curves).
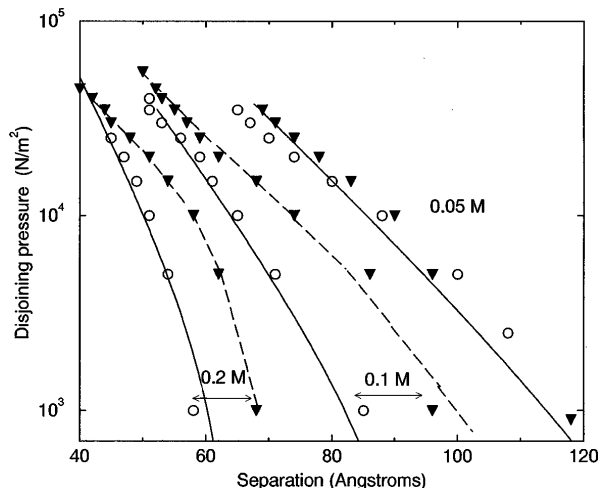

FIG. 3. Π_d-isotherms of free-standing films AOT (2.5 mM), with from the right to the left, a concentration of 0.05, 0.1, and 0.2 M of (circles) CsCl, and (triangles) LiCl; (solid lines) fits using Lipshitz theory for dispersion forces [21] and Poisson-Boltzmann equation for electrostatic forces [22] (dashed lines are guides to the eye).
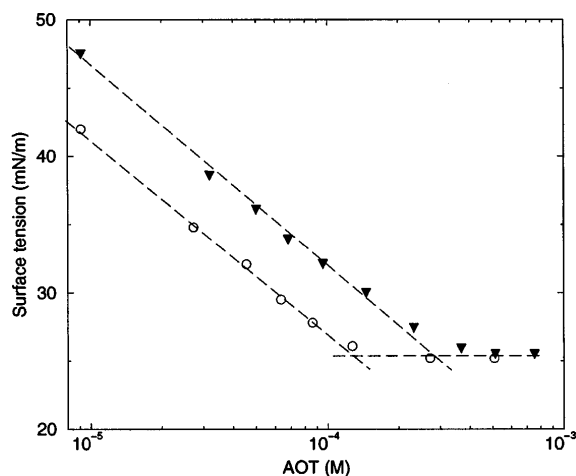
FIG. 4. Surface tension isotherms, measured with the Wilhelmy balance system, of AOT with added 0.2 M of (circles) CsCl and (triangles) LiCl. The CMCs are located at the intersection between the dashed lines.

CMC, finite size effects are not supposed to intervene. Therefore, the adsorption of AOT molecules will be hindered by the hydration shell of the Li^+ counterions that appears to weaken the electrostatic screening of the SO_3^- groups. Thus, a basic approach to explain the gap between the Π_d-isotherms would be an augmentation of the Debye screening length of the LiCl systems by reducing the net charge of the Li^+ counterions, induced by the local screening of the surrounding water molecules. On the other hand, one should also evaluate the dehydration energy cost of the Li^+ ions in the screening process of the SO_3^- groups. An interesting point is that at pressures $\gtrsim 10^4$ N/m^2 the gap between the Π_d-isotherms diminishes and the slope of the Li^+ Π_d-isotherms becomes lower than for Cs^+, which is consistent with an augmentation of the Debye screening length. Nevertheless, in this part of the Π_d-isotherms, and at these high ionic strengths, attractive ionic fluctuations may also be considered [5].

In conclusion, The deviations between the CsCl Π_d-isotherms and LiCL Π_d-isotherms are the signature of a hydration effect. We have shown that it is significant up to distances of ≈ 100 Å. Therefore, it appears that ion hydration phenomenon gives rise not only to structural short range forces but also, and similar to finite size effects, has a long range behavior. Its action may be understood within the framework of the electrostatic theory by considering the local screening of the hydrophilic ions by the surrounding water molecules.

*Present address: F.O.M. Institute, Kruislaan 407, 1098 SJ Amsterdam, The Netherlands.

[1] T. Kolarov, R. Cohen, and D. Exerowa, Colloids Surf. **42**, No. 1-2, 49 (1989).

[2] D.S. Dean and D. Sentenac, Europhys. Lett. **38**, 645 (1997).

[3] P. Guenoun, A. Schalchli, D. Sentenac, J.W. Mays, and J.J. Benattar, Phys. Rev. Lett. **74**, 3628 (1995).

[4] D. Exerowa, T. Kolarov, and Khr. Khristov, Colloids Surf. **22**, 171 (1987).

[5] D. Sentenac and D.S. Dean, J. Colloid Interface Sci. **196**, 35 (1997).

[6] D.S. Dean, R.R. Horgan, and D. Sentenac, J. Stat. Phys. **90**, 899 (1998).

[7] O. Bélorgey and J.J. Benattar, Phys. Rev. Lett. **66**, 313 (1991).

[8] J. Israelachvili, *Intermolecular and Surface Forces* (Academic Press, New York, 1992).

[9] E.J.W. Verwey and J.Th.G. Overbeek, *Theory of Stability of Lyophobic Colloids* (Elsevier, Amsterdam, 1948).

[10] I. Borukhov, D. Andelman, and H. Orland, Phys. Rev. Lett. **79**, 435 (1997).

[11] R. Kjellander and S. Marcelja, J. Phys. Chem. **90**, 1230 (1986).

[12] E.F. Williams, J. Colloid Sci., **12**, 452 (1957).

[13] K.J. Mysels and M.N. Jones, Discuss. Faraday Soc. **42**, 42 (1966).

[14] D. Exerowa and A. Scheludko, C.R. Acad. Bulg. Sci. **24**, 47 (1971).

[15] A. Schalchli, J.J. Benattar, and T. Kolarov, C.R. Acad. Sci. II Mec. Phys. Chim. Astron. **319**, 745 (1994).

[16] D. Sentenac, A. Schalchli, M. Nedyalkov, and J.J. Benattar, Faraday Discuss. **104**, 345 (1996).

[17] B.V. Derjaguin, N.V. Churaev, and V.M. Muller, *Surface Forces* (Consultant Bureau, New York, 1987).

[18] M. Born and E. Wolf, *Principles of Optics* (Pergamon, London, 1980).

[19] M.N. Jones, K. Mysels, and P.C. Scholten, Trans. Faraday Soc. **62**, 1336 (1966).

[20] R. Krustev, D. Platikanov, and M. Nedyalkov, Colloids Surf. A **123-124**, 383 (1997).

[21] W.A.B. Donners, J.B. Rijnbout, and A. Vrij, J. Colloid Interface Sci. **60**, 540 (1977).

[22] D.Y.C. Chan, R.M. Pashley, and L.R. White, J. Colloid Interface Sci. **77**, 283 (1980).